SEA ICE CLASSIFICATION USING COMBINED SENTINEL-1 AND SENTINEL-3 DATA

Stefan Wiehle[1], Dmitrii Murashkin[1], Anja Frost[1], Christine König[2], Thomas König[2]
1: German Aerospace Center (DLR), Maritime Safety and Security Lab Bremen, Germany
2: König und Partner Fernerkundung GbR, Dießen am Ammersee, Germany

ABSTRACT

We present a new approach for sea ice mapping based on Synthetic Aperture Radar (SAR) data from Sentinel-1 and an existing sea ice classification using optical-thermal data based on Sentinel-3. SAR and optical-thermal sensors provide different information about the sea ice situation: while SAR backscatter depends mainly on the topography of the sea ice surface and properties of the ice volume, optical sensors provide further information about the structure and moisture of ice and snow. In order profit from both sensors, a convolutional neural network (CNN) is trained with collocated images from both satellite missions. Compared to a pure SAR classification, the results of the combined approach show an improved classification reliability, especially in areas with open water.

Index Terms— Sea ice classification, SAR, SLSTR, data fusion, remote sensing

1. INTRODUCTION

Sea ice is an essential component of the Arctic environment. Its coverage and thickness play an important role in weather forecasting and the global climate system [1]. In addition, sea ice has significant impacts on human activities in the polar regions, such as shipping and offshore constructions. Therefore, mapping and classifying sea ice is an important task to ensure the safety and efficiency of human activities without harming the sensitive Arctic region, and to support studies on climate and environmental research.

As the polar regions are dark during winter time and, in particular, often covered by clouds, active microwave sensors such as Synthetic Aperture Radar (SAR) are a useful remote sensing tools for observing the polar sea ice and its evolution [1]. The data acquisition is generally unaffected by atmosphere, solar illumination, or clouds.

However, to analyze long-term changes in the sea ice and therefore handle large amounts of data efficiently, automatic algorithms for classifying the sea ice are required.

An abundance of approaches for SAR-based sea ice classification have been developed (e.g., [2]), summarized very comprehensively in [3]. Nevertheless, obtaining accurate classifications year-round is still a challenge. Different ice classes can show similar radar backscatter responses, which limits the performance of sea ice classification. Seasonally, the radar backscatter signal can be affected by precipitation: wet snow obscures information about underlying ice types [4] which results in misclassifications.

In order to overcome misclassifications, we utilize collocated classifications based on optical-thermal data from the Sea and Land Surface Temperature Radiometer (SLSTR) of Sentinel-3 satellite mission. SLSTR measures the reflected sunlight in different bands which also include thermal information. Figure 1 illustrates the general workflow of the two classification strategies we analyze in this paper. The Sentinel-3 based classification is sketched in Chapter 2. The pure SAR-based classification is then described in Chapter 3. Chapter 4 goes into the fused approach. Our test results shown in Chapter 5 compare the pure SAR-based classification with the fused classification. This test deals with 100 Sentinel-1 scenes and the same number of collocated Sentinel-3 classifications taken over the Arctic ocean.

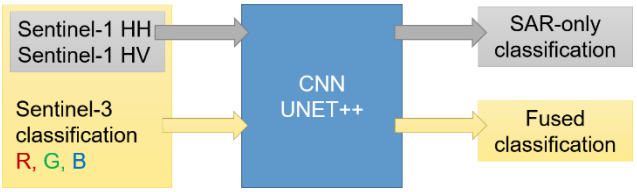

Figure 1: General data flow of the Sentinel-1 classification and the combined Sentinel-1/Sentinel-3 classification.

2. OPTICAL-THERMAL CLASSIFICATION

The Sentinel-3 SLSTR ice classification is an improved version of the ice differentiation algorithm presented in [5]. Improvements have been made in cloud detection and the development of an operational processing chain that enables faster and therefore more up-to-date information to be provided to maritime users.

The results of the algorithm are verified by comparing them with high-resolution optical remote sensing data, webcam recordings, the official sea-ice maps of ice services as well as the predictions of Canadian ice models. In addition to a wide field of view of approx. 1420 km, this pixel-based ice/snow classification has the ability to differentiate 17 classes with a resolution of 500 m in both Arctic and Antarctic. An example is shown in Figure 2.

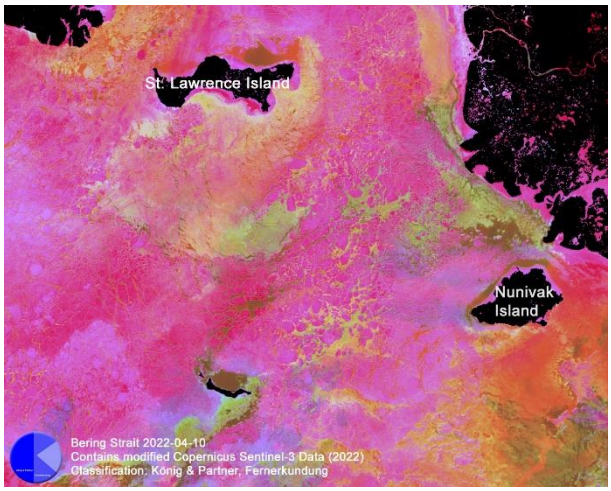

Figure 2: Sentinel-3 SLSTR Sea ice Classification from K&P, Bering Strait 2022-04-10

Figure 3: Legend for Sentinel-3 SLSTR sea ice classification of K&P

The output is an RGB color representation with smooth color transitions. Some of the main colors identified reflect classes ranging from open water to approximately 50 cm thick ice. Other colors could be assigned to snow surface properties, but without being able to determine specific ice thicknesses underneath. Figure 3 shows the complete legend. The reduction to the main colors is dispensed with at this stage, because this would result in important information being lost unnecessarily. In addition, the results provided are better suited as input data for a neural network.

If cloud cover is present in the SLSTR data, the representation is replaced by suitable shades of gray. In this process, two shades are reserved, namely (0,0,0) for land and (110,110,110) for background.

3. SAR CLASSIFICATION

The classification for SAR uses Sentinel-1 Extended Wide Swath (EW) data, since EW is the preferred mode acquired over arctic waters and, hence, most suitable for frequently updated sea ice information. The classification used herein is presented and explained in detail in [6].

After image preprocessing to reduce thermal noise, a Convolutional Neural Network (CNN) in a UNET++ architecture is applied for classification. This is outlined in Figure 4. Its input data are both channels of the Sentinel-1 EW mode (HH and HV) in tiles of 256x256 pixels. The encoder (red arrows) has a depth of six layers, whereas the decoder part (green arrows) has four layers. The column on the left shows the tile size at each depth level. Numbers in boxes show the input and the output tensor shapes.

The output is in four times lower resolution, significantly reducing the processing time. For the 40 m pixel spacing of Sentinel-1 EW GRDM (ground range detected, medium resolution) data, this results in 160 m resolution for the classification product.

The classifier distinguishes between six classes:

- Smooth open water and leads
- Rough open water and leads
- New ice (up to ~30 cm)
- First-year ice (up to ~1,5 m)
- Multi-year ice (>1,5 m)
- Rough ice (crushed ice, frost flower, ice ridges)

Since SAR only detects the surface of the sea ice, the stage of development (new, first-year, multi-year, rough) and associated thickness can only be derived from the surface roughness.

4. FUSED CLASSIFICATION

The fused classification uses collocated input from both satellite missions, Sentinel-1 and Sentinel-3, with the goal to combine both different types of information to a sophisticated, more accurate sea ice classification product. During our study, multiple options were considered to determine the setup and output of the fused classification, e.g.

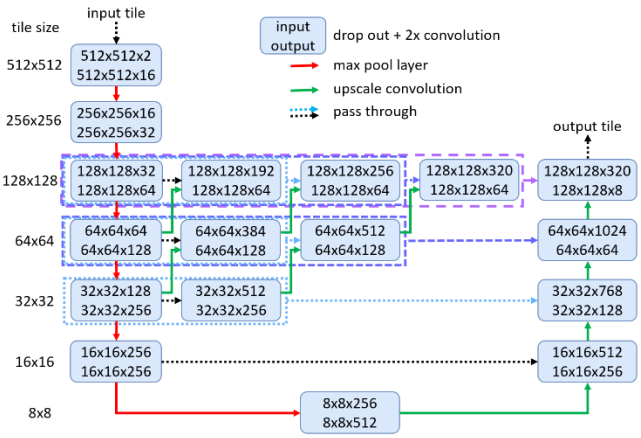

Figure 4: CNN model for the SAR sea ice classification based on UNET++ architecture.

classifying individually (as described in Sections 2 and 3), then combining both returned classes for each pixel. For the fusion presented here, we decided to use the Sentinel-1 data and the Sentinel-3 classification as input. Since the Sentinel-3 classification still contains information as it is not limited to only a handful of classes and is extensively validated, this is considered an advantage compared to using L1 Sentinel-3 data.

The fused classification uses a CNN in UNET++ architecture similar to the SAR classification. The input for the fusion consists of 5 channels: Sentinel-1 HH/HV and Sentinel-3 classification R/G/B. 150 manually labelled scenes were used in training.

For processing, SAR and optical-thermal datasets have to be collocated, meaning their coverage and resolution must be matched, so that they can be used as stacked channels within one image. Therefore, first the Sentinel-1 scenes are warped to the same Coordinate Reference System (CRS) as the Sentinel-3 classification. Next, the spatial overlap is calculated and both scenes are cut to this extend. Then the Sentinel-3 data is upsampled from 500 m pixel spacing to the Sentinel-1 pixel spacing of 40 m. Once both images are aligned, a validity mask is created and used in post processing to filter out land, clouds, and no-data areas at scene boundaries. Hence, the number of actually valid classified pixels can be much less than the common scene extent, depending on land presence, geometric conditions and cloud coverage. For consistency, we do not to add the SAR classification in cloud-covered areas in the fusion product, but provide data only where both sources have data available.

The temporal colocation between a SAR sensor acquiring at dusk/dawn and an optical sensor acquiring around noon is a challenge, since their acquisitions are usually several hours apart. For selecting scenes for the training data set, the maximum time difference was set to 12 hours. Since this resulted mostly in acquisition from the same day (either Sentinel-1 dawn and Sentinel-3 noon, or Sentinel-3 noon and Sentinel-1 dusk), the same limit could be set in operational use.

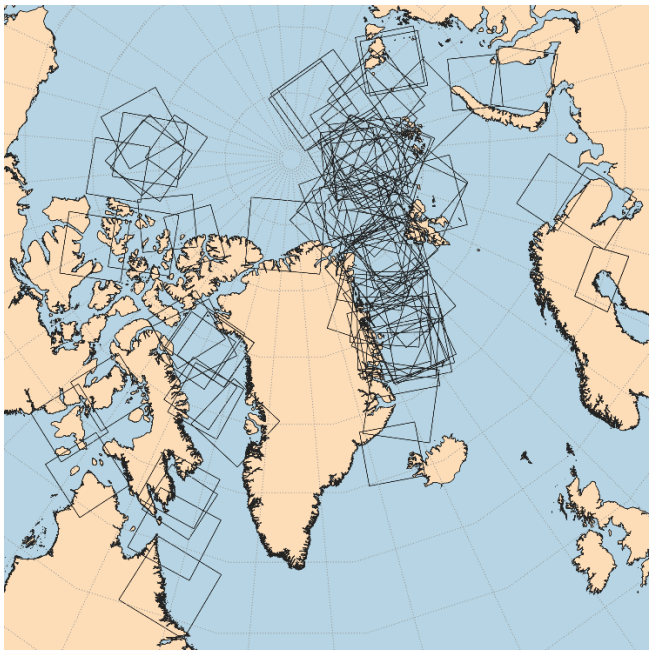

Figure 5: Overview of the 100 Sentinel-1 scenes used along with collocated Sentinel-3 classifications.

5. RESULTS

The SAR and fusion classifications were tested on a collection of 100 Sentinel-1 acquisitions and collocated Sentinel-3 classifications spread all over the Arctic, shown in Figure 5. Two examples of the classifications (SAR, optical, fused) are shown in Figure 6 and Figure *7*

In many cases, both classifications showed consistent results, mostly determining first-year ice as expected for many parts of the dataset. Occasionally, the fusion results tend to show older/thicker ice than SAR, but without SAR's frequent inclusion of small rough ice areas. This trend is visible in both Figs. 6 and 7. A possible explanation might be that the optical classification can only distinguish ice thicknesses up to ~50 cm and is sensitive also to snow cover, so first-year and multi-year ice are indistinguishable by the optical classification. Nevertheless, some of the features were apparently learned by the fusion CNN and result in an increased ice thickness estimate compared to the SAR-only classification. In other areas, on the other hand, such as the right part of Figure 7, the multi-year ice is reduced to first-year ice.

Figure 7 demonstrates an advantage for fusion when it comes to open water areas: The SAR classification shows several open water areas in the coastal inlets, where the sea ice appears dark in the SAR scene. In the fusion classification, these open water areas disappear, in agreement to the optical classification.

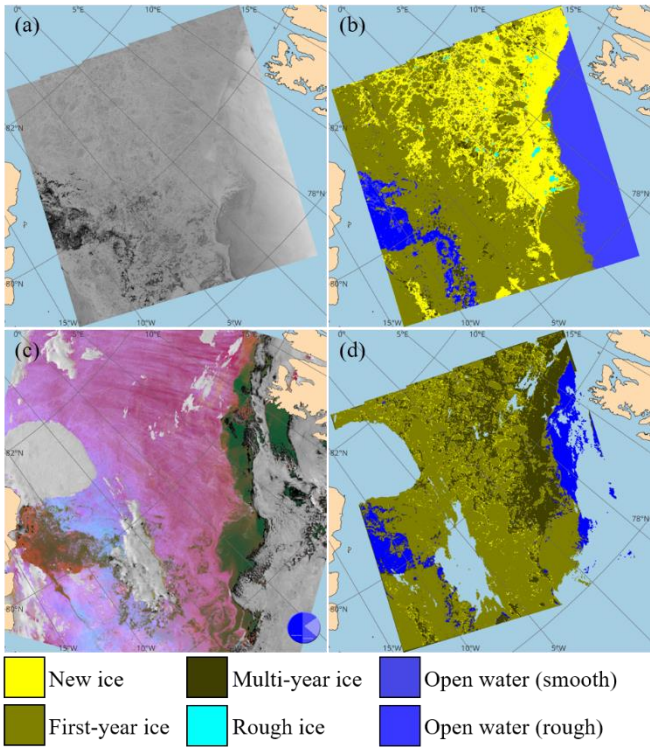

Figure 6: Example for a fused classification product from 2020-06-05 in the Fram Strait. (a) Sentinel-1 SAR scene, (b) SAR-only classification, (c) Sentinel-3 classification, (d) fused classification.

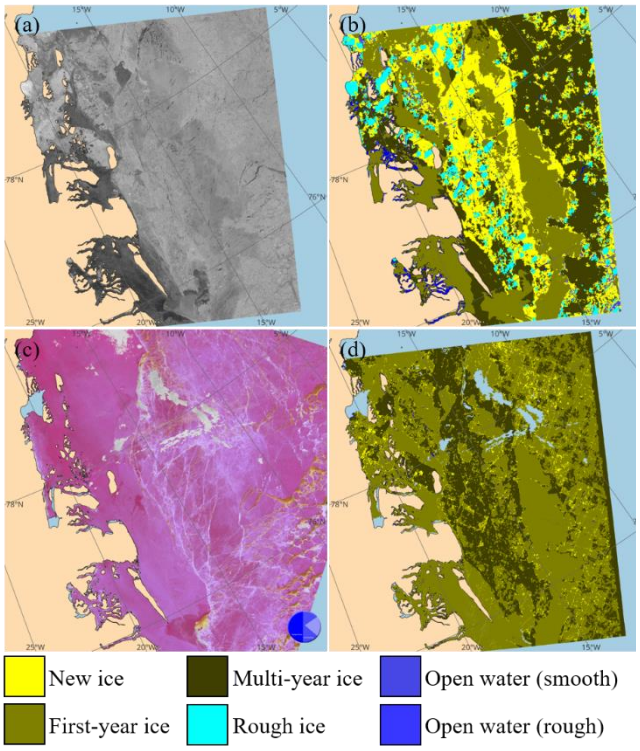

Figure 7: Example for a fused classification product from 2020-04-07 at the east coast of Greenland. (a) Sentinel-1 SAR scene, (b) SAR-only classification, (c) Sentinel-3 classification, (d) fused classification.

6. SUMMARY AND OUTLOOK

In this contribution, we present a sensor data fusion approach to improve the task of sea ice type classification. Two spaceborne sensors are used: SAR from Sentinel-1 and SLSTR from Sentinel-3. SAR and SLSTR data yield very different information about the sea ice situation. SAR backscatter depends mainly on sea ice surface roughness and topography, and the radar signals easily penetrate clouds. Optical sensors measure the reflected sunlight in different bands which, for SLSTR, also include thermal information. Both sensor sources are combined to form a fused classification, whereby the respective information is utilized. For this fusion, we use a CNN with a UNET++ architecture.

Our results show that in their current status, most areas align well between the classifications and open water is better distinguished in the fusion classification. In some areas, the fusion classification is likely overestimating the true sea ice thickness. Further training could improve this behavior. However, judging the correct classification is a challenge in the remote Arctic areas due to the lack of true ground truth data.

Other approaches for fusion on a product level might be considered in future work, e.g., Kalman filter or Bayesian networks.

The time difference between the SAR and optical acquisitions may cause inconsistencies in the observed sea ice situation caused by sea ice drift. In retrospect, a sea ice drift compensation such as presented in [7,8] can be included to enable the fusion of several sequential SAR acquisitions and stabilize the classification. For near real-time applications, an approach to compensate for this is to morph the respective scenes or classifications using sea ice drift forecast model data [9].

The classifications presented here are integrated in an operational processing chain and an end-user application specifically developed for the use aboard of polar operating ships (icysea.app developed by Drift & Noise Polar Systems). This contributes to the safety of scientific and commercial shipping in ice-infested waters.

ACKNOWLEDGEMENTS

The work described herein was carried out in the scope of the BMDV-funded mFUND project EisKlass2, FKZ 19F2122A. Figures 2, 6 and 7 contain modified Copernicus Sentinel-1 and Sentinel-3 data, 2020 and 2022.

REFERENCES

[1] Onstott, R. G., & Shuchman, R. A. (2004). “SAR measurements of sea ice”. Synthetic Aperture Radar Marine User’s Manual. Washington, DC: NOAA, 81-115.

[2] Ressel, R., Frost, A., & Lehner, S. (2015). “Navigation assistance for ice-infested waters through automatic iceberg detection and ice classification based on TerraSAR-X imagery”. The International Archives of Photogrammetry, Remote Sensing and Spatial Information Sciences, 40(7), 1049.
[3] Zakhvatkina, N., Smirnov, V., & Bychkova, I. (2019). “Satellite SAR data-based sea ice classification: An overview”. Geosciences, 9(4), 152.
[4] Kortum, K., Singha, S., & Spreen, G. (2022). „Robust Multiseasonal Ice Classification From High-Resolution X-Band SAR”. IEEE Transactions on Geoscience and Remote Sensing, 60, 1-12.
[5] C. König, T. König, S. Singha, A. Frost, and S. Jacobsen, “Combined Use of Space Borne Optical and SAR Data to Improve Knowledge about Sea Ice for Shipping,” Remote Sensing, vol. 13, no. 23, 2021
[6] D. Murashkin and A. Frost, “Arctic Sea ICE Mapping Using Sentinel-1 SAR Scenes with a Convolutional Neural Network,” In 2021 IEEE International Geoscience and Remote Sensing Symposium IGARSS, 2021, pp. 5660–5663.
[7] Wiercioch, M., Frost, A., & Singha, S. (2019).”Superposition of Sea Ice Classification Based on Synthetic Aperture Radar Images Considering Underlying Drift”. In IEEE International Geoscience and Remote Sensing Symposium IGARSS 2019, pp. 4206-4209. IEEE.
[8] Frost, A., Imber, J., Murashkin, D., Gregorek, D., & Bathmann, M. (2023). “Phase-Correlation Based Sea Ice Motion Tracking and Classification Using Spaceborne SAR Imagery”. In OCEANS 2023-Limerick. IEEE.
[9] Bathmann, M., Murashkin, D., Schmitz, B., Frost, A., Wiehle, S., Ludwig, V., Spreen, G. (2023). „Sea Ice Data for Shipping Routes”. AGU23, 2023-12-11 - 2023-12-15, San Francisco, CA, USA